

Research Article

Comparison of Photoelectrochemical Current in Amorphous and Crystalline Anodized TiO₂ Nanotube Electrodes

Candy C. Mercado , Michael Eric L. Lubrin, Hazel Anne J. Hernandez, and Reynaldo A. Carubio Jr.

Department of Mining, Metallurgical, and Materials Engineering, College of Engineering, University of the Philippines, Diliman, Quezon City 1101, Philippines

Correspondence should be addressed to Candy C. Mercado; ccmercado1@up.edu.ph

Received 17 January 2019; Revised 13 March 2019; Accepted 10 April 2019; Published 16 May 2019

Guest Editor: Hongmei Luo

Copyright © 2019 Candy C. Mercado et al. This is an open access article distributed under the Creative Commons Attribution License, which permits unrestricted use, distribution, and reproduction in any medium, provided the original work is properly cited.

The interest in TiO₂ nanotubes has resulted in a lot of studies including the effects of various parameters on the properties and performance for different applications. This study investigated the effect of anodization at a low temperature on the properties and photoelectrochemical performance. The effects of varied anodization settings on morphology, crystallinity, and PEC response were studied. Low-temperature anodization resulted in smaller pore diameter and shorter tube length. Annealing temperature affected the presence of varied phases of TiO₂ such as the prominence of anatase and amounts of rutile and amorphous TiO₂ at 125°C. To observe photoelectrochemical response, annealing at 450°C is necessary. However, a cathodic response was observed for TiO₂ nanotubes synthesized with low voltage at low temperature. Hence, amorphous titania nanotubes annealed at 125°C with thickness achieved in the anodization can be a potential material used for photocatalytic applications due to its determined cathodic photoelectrochemical response.

1. Introduction

Titanium dioxide (TiO₂) has been used in various applications such as biomedical devices, solar cells, and photodegradation [1–4]. TiO₂ nanotubes (NTs), in particular, are utilized due to their tube-like configuration that exhibits high surface area, relatively short conduction path [3, 5], and biocompatibility [4, 6].

TiO₂ has three main phases, namely, anatase, rutile, and brookite. As-synthesized titania via anodization occurs as amorphous [1] and transforms to various phases during additional heat treatments done after synthesis. Anatase transforms irreversibly to rutile at a process temperature that ranges from 400°C to 1200°C, depending on the raw material and processing methods applied [1, 7]. Anatase shows photoelectrochemical property and is used for photoelectrolysis applications such as water splitting and catalytic photodegradation through the presence of various active surfaces and defects [8, 9]. Hydrophilicity of TiO₂ is thought to aid with

the kinetics of both reactions, and amorphous titania has shown a comparable hydrophilic response after surface treatment to anatase [7].

In this study, we have selected a method that will allow us to compare the crystalline and amorphous structures of TiO₂ NTs produced by anodization of titanium. Various methods have been developed to synthesize TiO₂ NTs; one of these methods is anodic oxidation (anodization). Anodization is a low-cost electrochemical process that produces ordered or highly aligned oxide nanotubes or pore structures on a substrate by immersion in an acid electrolyte solution at room temperature and subsequent application of electric current. An additional step of annealing or heat treatment on the synthesized nanotubes is done in order to remove impurities and to change the crystal structure of the TiO₂. Annealing TiO₂ at 400°C leads to the transformation of the crystal structure to anatase TiO₂, while heat treatment at 800°C produces a rutile crystal structure of TiO₂ [7].

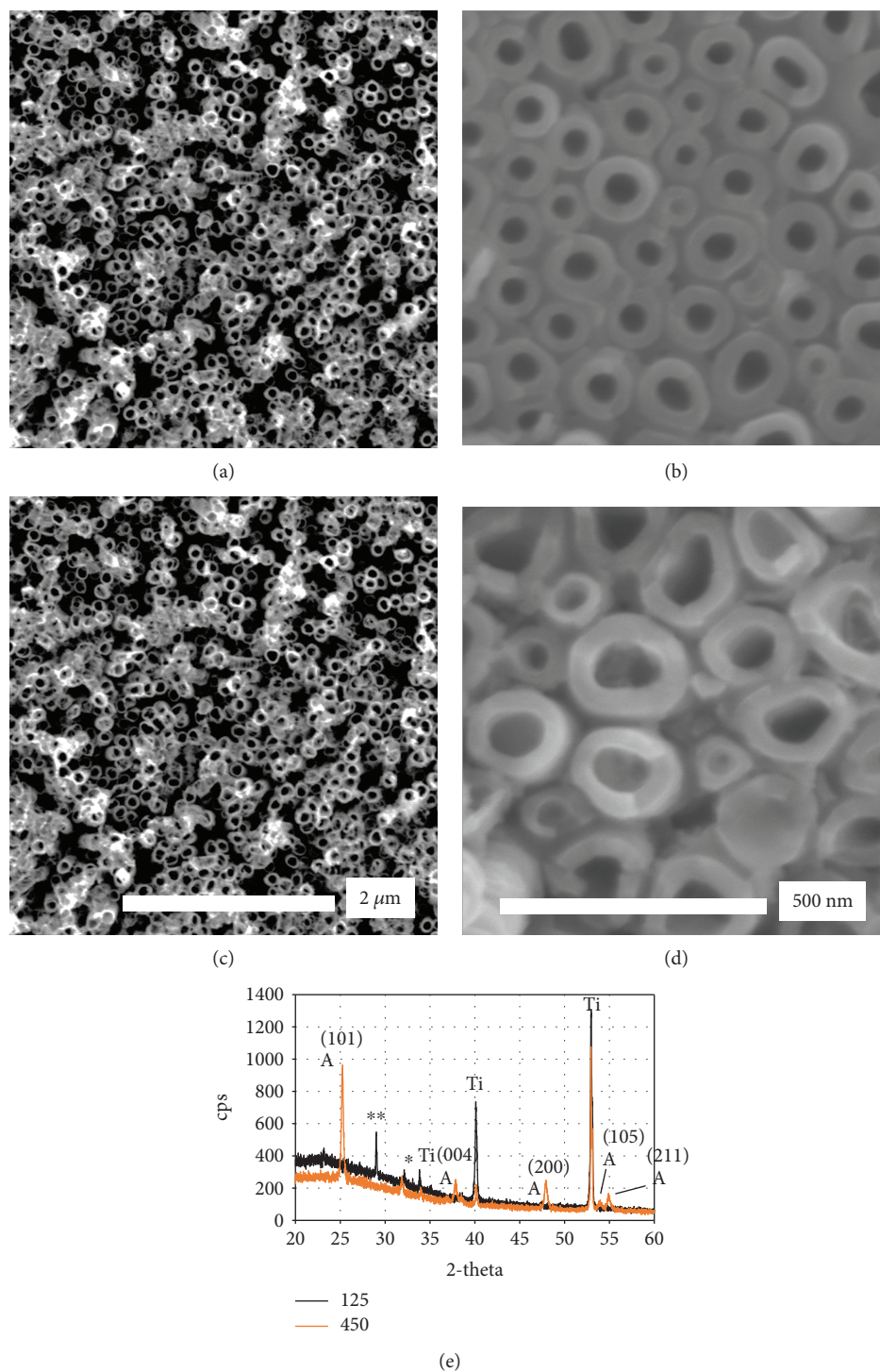


FIGURE 1: Scanning electron microscope images of 40 V RT grown nanotubes annealed at (a, b) 125°C and (c, d) 450°C. The 2 μm scale bar is for (a, c) while the 500 nm scale bar is for (b, d). (e) X-ray diffraction patterns of the samples. ** indicates possible presence of carbon impurities after 125°C heating, while * is a possible other titanium oxide form.

The exposure of TiO₂ nanotubes to ultraviolet radiation produces highly oxidative holes and weakly reductive electrons [10]. Recent studies have measured the photoelectrochemical activity of anatase TiO₂ [3]. However, only a few studies have been conducted to determine the possible use of an amorphous TiO₂ as a source of these charges and as the medium for charge transport.

This study determines the photoelectrochemical activity of low-temperature synthesized TiO₂ nanotubes based on the photoresponse under dark and illuminated conditions. At present, annealing at high temperatures is necessary to achieve an anatase structure with a high degree of ordering. However, anodization at low temperature is known to suppress the mobility of ions resulting in enhanced self-order

at the expense of increasing thickness and pore diameter. Moreover, synthesis at such condition can exhibit photore-sponse as reported in this paper.

2. Experimental

The method for anodization of titanium has been published in several papers [1]. The detailed method is as follows: the electrolyte consisted of 200 mL of ethylene glycol with 2% vol. H_2O and 0.09 M of NH_4F . High-purity (99.99%) titanium foil was polished with a 1200-grit size SiC paper and was used as substrate. The substrate was subjected to ultra-sonic cleaning with distilled H_2O and then air-dried. There were two types of anodization set-up used for this experiment: one was done at room temperature, 27°C , while the other one was at a lower temperature of approximately 5°C and with the temperature maintained by using an ice bath. The electrodes had a constant spacing of 1 cm. Changes in current over time during the anodization were monitored during potentiostatic anodization. A preliminary potentiostatic anodization set-up was connected to a potentiostat instead of a DC power supply for testing the chronoamperometric plot of the anodization process at 10 volts. Data were collected at 10 V and 5 V from this test.

Ti foils were imaged using a field emission scanning electron microscope (FESEM) with energy-dispersive X-ray (EDX) for chemical identification and quantification. The structure of the anodized TiO_2 was characterized using X-ray diffraction (XRD) with $\text{Cu K}\alpha$ radiation ($\lambda = 0.154 \text{ nm}$), at the scanning range $2\theta = 20^\circ - 60^\circ$. The phases were identified by comparing the peak data to reference single crystal data of R070582 (anatase), R050363 (brookite), R040049 (rutile), and 0011195 (titanium).

Three-electrode electrochemical cell was utilized with TiO_2/Ti as the working electrode, Pt as the counter electrode, and Ag/AgCl as the reference electrode. The spacing between the working and counter electrodes was maintained at 1 cm. The set-up used 1.0 M aqueous solution of Na_2SO_4 as the electrolyte and was connected to a potentiostat. Chronoamperometry was done by running the set-up in different voltages (-0.5 V , 0 V , and 0.5 V) with discontinuous illumination from the 10 W LED light source. The illumination was turned on and off at the interval of approximately 1 to 5 minutes to allow the electrolyte-electrode interface to equilibrate. Data were averaged after plotting as part of data analysis.

3. Results and Discussion

The formation of nanotubes was monitored by measuring the current during anodization as a function of time. The measurements were carried out at two different voltage settings, 5 V and 10 V, with current-time curves obtained during the anodization shown in Figure S1. A drastic drop in the current was observed in the early stages of anodization for both voltage settings, corresponding to the initial passivation of Ti foil leading to the formation of the barrier oxide layer. The formation of the barrier layer was governed by the oxidation of Ti to Ti^{4+} and its reaction to O^{2-} that was

TABLE 1: FWHM of XRD peak (101) at different anodization voltages. Samples were anodized at room temperature and annealed at 450°C .

Anodization voltage (V)	FWHM ($^\circ$)
30	0.38
40	0.44
50	0.58

produced by the deprotonation of H_2O upon the introduction of an electric field; the progress of the reaction caused an exponential decrease in the field strength on the Ti foil, leading to a barrier layer of finite thickness. After the initial current drop, a slight increase in current was observed at 10 V anodization. This indicated the initiation of pits that served as the precursor of the nanotubes [11]. This stage was not observed on 5 V anodization where gradual reduction followed the initial drop in current. It can be said that the pitting potential needed for nanotube formation lies between 10 V and 5 V. Under similar electrolyte characteristics, nanotubes are expected to form at operating voltages of 30 V, 40 V, and 50 V. The last stage of anodization was characterized by a gradual decrease in current until the quasi-steady state is reached. This indicated the continued formation of the nanotubes through the increase in nanotube length. At this stage, the nanotubes competed with each other until a condition of equal sharing of available current is achieved, leading to appreciable self-ordering of nanotubes as seen in the SEM images of the nanotubes in Figures 1(a)–1(d). Formation of TiO_2 nanotubes was a result of the competition between the oxidation of the Ti substrate and the etching or dissolution of the formed oxides by the fluoride ions present in the electrolyte [2].

As-synthesized TiO_2 nanotubes did not show ordered crystal structures as shown in Figure 1(e). These amorphous tubes undergo phase transformation at elevated temperatures, crystallizing to form titania polymorphs like anatase and rutile as shown in various studies [1]. In the study by Poulomi et al., XRD patterns showed that anatase started to form at around 280°C but annealing operations are usually done at 450°C to ensure an adequate amount of anatase with few rutile phases [1]. Moreover, further increase in temperature promoted the transformation to rutile phase and started to dominate at a temperature range of 500°C – 600°C [1]. Figure 1(e) shows the X-ray diffraction pattern of the samples annealed at 125°C and 450°C . The anatase peaks are visible for the 450°C annealed sample but not in the 125°C annealed sample. A shift into the lower intensity of the broad baseline at 2θ from 20° to 35° indicated conversion of the phase from amorphous to crystalline. Annealing at 450°C resulted in a structure dominated with anatase phase and with minimal rutile phase. The anatase phase has a strong preferential orientation at the (101) plane. The crystallinity in each voltage setting was determined by the full-width half-maximum values for the (101) plane where full-width half-maximum (FWHM) trends, given in Table 1, showed increasing crystallinity with anodization voltage.

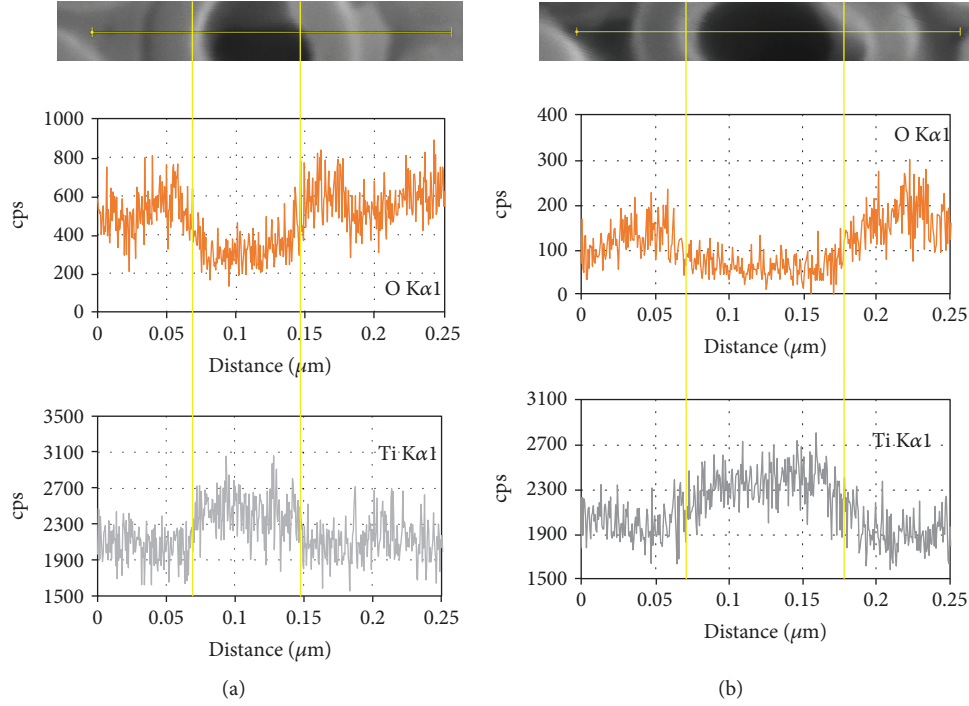


FIGURE 2: EDX linescan along the diameter of the tube showing oxygen and titanium distributions for (a) sample 125°C and (b) 450°C samples.

The XRD patterns of the TiO_2 NTs synthesized at various anodizing voltages and post-heat-treated at different temperatures are illustrated in Figure S4. It can be seen that no crystalline titania phases were present at nanotubes that were post-heat-treated at 125°C. The TiO_2 NTs synthesized via the anodization process were reported to be amorphous in nature [1]. From XRD, the anatase phase was only present at samples post-heat-treated at 450°C. In addition, rutile phases were also present at samples post-heat-treated at 450°C similar to other reports showing TiO_2 NTs heat-treated at 350°C to 450°C consisting of a rutile bottom layer and anatase tube walls [12].

Scherrer's formula shows the inverse proportionality of the peak width and crystallite size [13–15]. This was applied to the FWHM of the (101) anatase plane peak to calculate the crystallite size for the synthesized titania nanotubes that were post-heat-treated at 450°C. There have been differences in opinion in literature in the use of the Scherrer equation to determine the absolute crystallite size of nanoparticles [13, 16]; however, the trends of nanocrystal size and the peak width have shown good agreement in many instances [13]. Through this analysis, the increasing crystallinity of the nanotubes with annealing was supported by the decrease in peak width.

Stoichiometry was also varied after the 125°C and 450°C annealing. Figure 2 shows the EDX of a tube, with a line scan along the diameter, plotting the oxygen and titanium signals. The percentage of O and Ti in the tube was taken and showed approximately 3:2 Ti:O ratio for the amorphous TiO_2 and 3:1 for anatase TiO_2 . This was an averaged measurement and did not reflect the actual stoichiometry of the nanotube walls as the Ti signal from the tube holes was stronger

TABLE 2: Effect of the heat treatment post annealing for 40 V, room temperature anodized sample.

Annealing Temperature (°C)	Ti (wt.%)	O (wt.%)	Ti:O ratio
125	55	36	3:2
450	60.5	19	3:1

Note: X-rays from titanium metal substrate included in Ti wt.%.

TABLE 3: Energy-dispersive X-ray intensities (cps) for samples processed at different temperatures.

	Ti $L_{\alpha 1,2}$ (452.2 eV)	Ti $K_{\alpha 1}$ (4510.8 eV)	Ti $K_{\beta 1,3}$ (4931.8 eV)	O $K_{\alpha 1,2}$ (524.9 eV)
125-a	6.0	22.5	3.05	10
125-b	6.0	22.5	2.95	10.1
450-a	2.0	21.35	2.9	2.4
450-b	2.3	20.0	2.65	3.2

(signals originating from the substrate). However, relative amounts of Ti and O showed that prior to annealing, nanotubes were more oxygen-rich (Table 2).

Aside from semiquantitative chemical compositions, the EDX signal was also analyzed for the element environment [17]. The basis of this analysis is that in amorphous materials, the neighboring atoms are not arranged in a lattice and could have different nearest neighbor environments compared to other atoms within the same phase. In crystalline, anatase gives a different type of titanium environment [18]. From literature, the environment of an atom can be distinguished

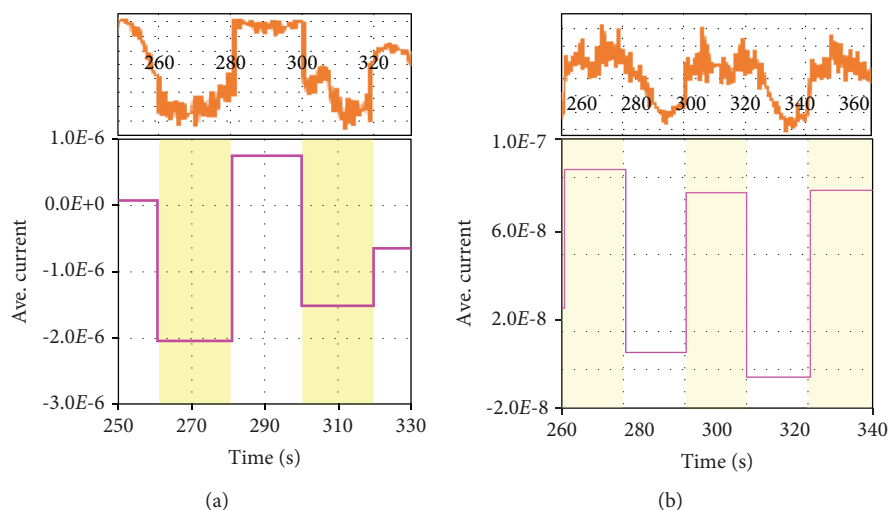


FIGURE 3: Chopped-illumination chronoamperometry (CA) for sample 30 V LT 450°C with polarization (a) -0.5 V vs. Ag/AgCl. In this figure and up to the end, the data is shown in the inset while the average value is shown as horizontal lines; shaded regions indicate illuminated portions of the measurements.

from the ratio of the K_α and K_β peaks of the EDX signal. In the nanotube samples, there were two spots measured (Table 3); a larger difference between Ti K_α /Ti K_β ratios was seen in the amorphous nanotubes. These stoichiometric differences between environments in amorphous TiO_2 lead to the formation of a range of defects. Predominant defects studied in literature are oxygen vacancies and Ti^{3+} sites. Excess oxygen in amorphous TiO_2 indicates disordered Ti-O octahedra and tetrahedra that may lead to oxygen-rich surfaces. Theoretical studies by Pham and Wang have shown that the formation of oxygen vacancies requires less energy in amorphous TiO_2 [19]. These vacancies then form defect channels for carrier transport contributing to amorphous conduction.

Nanotube dimensions are a few of the factors that affect the photoelectrochemical activity of nanotubes; hence, it is crucial to measure them. Images of TiO_2 nanotubes synthesized at room temperature and low-temperature anodization annealed at 450°C are shown in Figure S2. Based on the micrographs, dimensions such as pore diameter and wall thickness were determined. Measured pore diameters were averaged and plotted against anodizing potential (voltage) as shown in Figure S3. At room temperature anodization, pore diameters ranged from 88 to 120 nm, while at low-temperature anodization, relatively smaller pore diameters ranging from 62 to 120 nm were measured. Generally, a linearly increasing trend in pore diameters with increasing applied potential was observed for both room temperature and low-temperature anodization; similar trends were seen in other studies [20]. Varying the electrolyte temperature changed the conditions of the anodization reaction in terms of chemistry and thermodynamics. An increase in the electrolyte temperature leads to a decrease in the mass transport of the electrolyte and the species necessary for anodization [21].

Average TiO_2 nanotube wall thicknesses were also determined and plotted against the applied potential; comparison

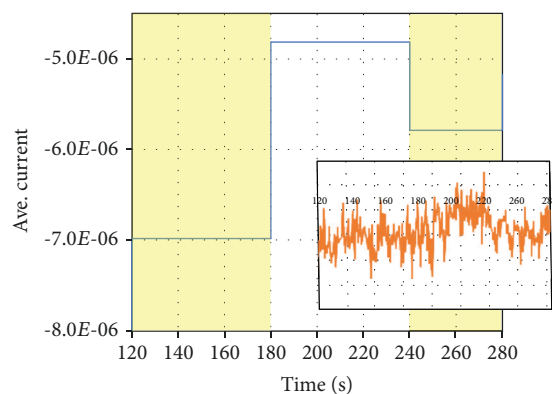


FIGURE 4: Photoresponse of the 30 V RT 125°C sample biased -0.5 V vs. Ag/AgCl during chopped-light measurement.

of all dimensions is shown in Figure S3. From Figure S3, it can be observed that a higher applied potential yields longer nanotubes. It has been shown that increasing the electric field strength resulted in a localized temperature rise across the oxide films due to the enhanced joule heating, resulting in the acceleration of nucleation of the oxides, faster growth, and consequent increase in thickness of the anodized films [6].

The photoelectrochemical activity of the nanotubes was analyzed by chronoamperometric measurements under discontinuous illumination. The three-electrode cell was allowed to stabilize prior to being operated for alternating on-off cycles at -0.5, 0, and 0.5 V versus Ag/AgCl. The current values obtained were divided by the active surface area during testing. The responses in terms of an increase or decrease in current density upon illumination were monitored for all samples. Good photoresponses were recorded for samples that were annealed at 450°C for both room temperature and low-temperature anodization. Generally, annealed samples show cathodic photoresponses upon illumination at applied bias -0.5 V (Figures S5–S7). When

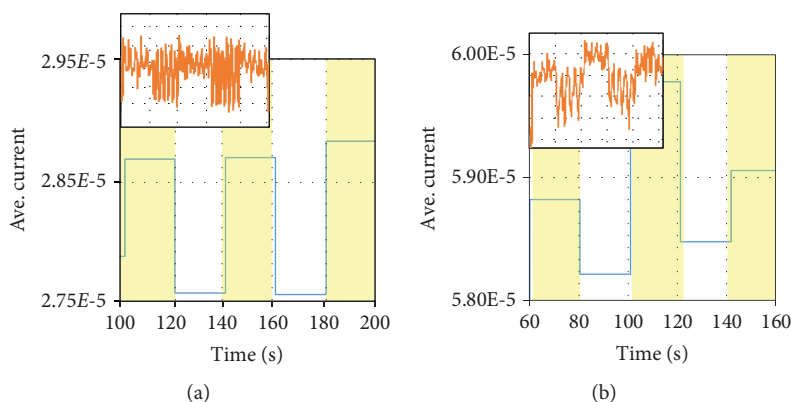


FIGURE 5: Oscillations in the measured current during chopped-light CA for 30 V RT 450°C sample with polarization (a) 0 V vs. Ag/AgCl and (b) 0.5 V vs. Ag/AgCl (other polarization settings failed to get stable current measurement).

0.5 V was applied, the plots registered anodic response as shown by the increase in current density under illumination (Figure 3).

For samples heat-treated at 125°C, photoresponses were not apparent and no clear distinction on the on and off regions of the graphs was observed. Details of the generated plots from 450°C and 125°C heat treatment temperature are shown in Figures S5 and S6. In a study by Beranek et al. on as-formed amorphous tubes, photocurrent generation is highly localized at the bottom of the tubes and is negligible for nanotube walls [22]. This is due to the presence of numerous defects in amorphous nanotubes that lead to poor charge transport [22]. Annealing at elevated temperature activated the walls of the nanotube as anatase structures crystallize, with anatase having the most efficient electron transport among the phases of TiO₂ [23].

One clear exception to these observations was the observed photocurrent of the 30 V, room temperature anodized nanotubes that were annealed at 125°C. The photoresponse of the nanotubes when the applied bias was -0.5 V is shown in Figure 4. Cathodic responses were recorded when the light was introduced. However, this observation was not seen in TiO₂ NTs. Although amorphous, a short-range order may be present in the sample and could result in shallow or deep electron and hole traps. This short-range order was not seen in X-ray diffraction patterns. Because of the direction of the measured photocurrent and considering that the illumination is composed of visible wavelengths, the defects were speculated as shallow electron traps. Cathodic behavior has been seen in some amorphous oxide of metals like iron-zirconium [24]. This occurrence is explained through the Poole-Frenkel process where the conduction was enabled by thermal ionization of trapped charges [25, 26]; in the case of the photocurrent observed in this sample, trapped charges with trap levels with higher binding energies are excited to the conduction band by light.

At constant anodization temperature, a decreasing trend in the current density was observed as the anodization voltage is increased from 30 V to 50 V (Figure S7). The observed trend was attributed to the measured crystallite sizes. Smaller grain size indicated abundance in grain boundaries within the nanotubes. It was theorized that these grain boundaries

impede the charge transport in the nanotubes. Thus, lower values were expected to be obtained for the 50 V anodized nanotube sample as this had the smallest crystallite size among the three anodization voltage settings.

Higher magnitudes for the current density were recorded for samples anodized at room temperature (Figure S7). This can be observed for annealed samples at all the anodization voltage settings. This was attributed to better nanotube dimensions for samples anodized at room temperature. It is important to note that while smaller pore diameters were obtained for low temperature which suggests that more nanotubes can fit on a specific unit area, the lengths of the nanotubes were shorter relative to that of room temperature anodized nanotubes.

Current oscillations were seen in 30 V room temperature anodized samples that were annealed at 450°C (Figure 5). From several papers that have explored the origin of this sinusoidal current, reasons for this were chemical oscillations—localized areas of reactions within the entire surface of the electrode [27], nonlinear transport [28], and nonplanarity of the electrode surface as in this case. In the case of the three-electrode system with TiO₂ WE, Pt CE, and Ag/AgCl RE, oscillations occurred in the order of 1 μ A.

The photocurrent was recorded to be higher in room temperature anodized sample compared to low-temperature anodized sample for the sample anodization voltage; taking into consideration the difference in the nanotube length and getting photocurrent density considering the nanotube thickness (photocurrent/volume), similar photocurrents were observed. This could indicate that in photoelectrochemical measurements, the total surface area of the nanotubes determines the generated photocurrent, even at the order of around 10 μ m thickness.

4. Conclusions

Cathodic and anodic photocurrents were seen (with -0.5 V and 0.5 V vs. Ag/AgCl, respectively) during chronoamperometric testing under discontinuous illumination. A -0.5 V bias promoted electron transport while 0.5 V bias promoted hole transport. Annealing at 450°C is necessary for effective photoresponse; however, cathodic photoresponse was seen

on nanotubes anodized at 30 V with an applied voltage of -0.5 V. This deviation was attributed to a short-range order and the occurrence of high oxygen surfaces that could form oxygen vacancies that are pathways of charge transport. The magnitude of current density decreased as the anodization voltage was increased due to the decreasing crystallinity when anodized with increasing voltage. The higher density of grain boundaries on nanotubes anodized at higher voltage may have hindered effective charge transport leading to a low-magnitude photoresponse. The photocurrent was observed in all annealed anatase samples. TiO_2 in the anatase phase has been known to be an efficient photoanode; through this experiment, it was seen that TiO_2 amorphous showed potential to be a photocathode in photoelectrochemical cells.

Data Availability

The data used to support the findings of this study are available from the corresponding author upon request.

Conflicts of Interest

The authors declare that they have no conflicts of interest.

Acknowledgments

The morphological analysis portion of this work was supported by the Department of Science and Technology (PCIEERD-ADMATEL/EPDC) with Albert Guevarra and Kim Christian Aganda, and the University of the Philippines System (OVPA-BPhD-2016-17) supported spectroscopy and modelling. CCM thanks Dr. Balela, Dr. Mena, Dr. Vasquez, and the Department of Mining, Metallurgical, and Materials Engineering of the University of the Philippines–Diliman for the use of various laboratory equipment. The authors also acknowledge the support of DOST and the Engineering Research and Development for Technology (ERDT) in the publication of this research.

Supplementary Materials

Details of electrochemical measurements and scanning electron microscope images with measurements derived from SEM images. (*Supplementary Materials*)

References

- [1] P. Roy, S. Berger, and P. Schmuki, "TiO₂ nanotubes: synthesis and applications," *Angewandte Chemie International Edition*, vol. 50, no. 13, pp. 2904–2939, 2011.
- [2] M. Szkoda, A. Lisowska-Oleksiak, K. Grochowska, Ł. Skowroński, J. Karczewski, and K. Siuzdak, "Semi-transparent ordered TiO₂ nanostructures prepared by anodization of titanium thin films deposited onto the FTO substrate," *Applied Surface Science*, vol. 381, pp. 36–41, 2016.
- [3] H. Kim, J. Khamwannah, C. Choi, C. J. Gardner, and S. Jin, "Formation of 8 nm TiO₂ nanotubes on a three dimensional electrode for enhanced photoelectrochemical reaction," *Nano Energy*, vol. 2, no. 6, pp. 1347–1353, 2013.
- [4] K. Das, S. Bose, and A. Bandyopadhyay, "TiO₂ nanotubes on Ti: influence of nanoscale morphology on bone cell-materials interaction," *Journal of Biomedical Materials Research Part A*, vol. 90A, no. 1, pp. 225–237, 2009.
- [5] C. C. Mercado, F. J. Knorr, and J. L. McHale, "Observation of charge transport in single titanium dioxide nanotubes by micro-photoluminescence imaging and spectroscopy," *ACS Nano*, vol. 6, no. 8, pp. 7270–7280, 2012.
- [6] Y.-T. Sul, C. B. Johansson, Y. Jeong, and T. Albrektsson, "The electrochemical oxide growth behaviour on titanium in acid and alkaline electrolytes," *Medical Engineering and Physics*, vol. 23, no. 5, pp. 329–346, 2001.
- [7] L. Yang, M. Zhang, S. Shi et al., "Effect of annealing temperature on wettability of TiO₂ nanotube array films," *Nanoscale Research Letters*, vol. 9, no. 1, p. 621, 2014.
- [8] F. J. Knorr, C. C. Mercado, and J. L. McHale, "Trap-state distributions and carrier transport in pure and mixed-phase TiO₂: influence of contacting solvent and interphasial electron transfer," *The Journal of Physical Chemistry C*, vol. 112, no. 33, pp. 12786–12794, 2008.
- [9] C. C. Mercado, F. J. Knorr, J. L. McHale, S. M. Usmani, A. S. Ichimura, and L. V. Saraf, "Location of hole and electron traps on nanocrystalline anatase TiO₂," *The Journal of Physical Chemistry C*, vol. 116, no. 19, pp. 10796–10804, 2012.
- [10] M. Tian, S. S. Thind, S. Chen, N. Matyasovzsky, and A. Chen, "Significant enhancement of the photoelectrochemical activity of TiO₂ nanotubes," *Electrochemistry Communications*, vol. 13, no. 11, pp. 1186–1189, 2011.
- [11] J. M. Macak, H. Tsuchiya, A. Ghicov et al., "TiO₂ nanotubes: self-organized electrochemical formation, properties and applications," *Current Opinion in Solid State and Materials Science*, vol. 11, no. 1-2, pp. 3–18, 2007.
- [12] S. P. Albu and P. Schmuki, "TiO₂ nanotubes grown in different organic electrolytes: two-size self-organization, single vs. double-walled tubes, and giant diameters," *Physica Status Solidi (RRL) - Rapid Research Letters*, vol. 4, no. 8-9, pp. 215–217, 2010.
- [13] A. Monshi, M. R. Foroughi, and M. R. Monshi, "Modified Scherrer equation to estimate more accurately nanocrystallite size using XRD," *World Journal of Nano Science and Engineering*, vol. 2, no. 3, pp. 154–160, 2012.
- [14] A. L. Castro, M. R. Nunes, A. P. Carvalho, F. M. Costa, and M. H. Florencio, "Synthesis of anatase TiO₂ nanoparticles with high temperature stability and photocatalytic activity," *Solid State Sciences*, vol. 10, no. 5, pp. 602–606, 2008.
- [15] K. Zhu, N. R. Neale, A. Miedaner, and A. J. Frank, "Enhanced charge-collection efficiencies and light scattering in dye-sensitized solar cells using oriented TiO₂ nanotubes arrays," *Nano Letters*, vol. 7, no. 1, pp. 69–74, 2007.
- [16] N. S. Gonçalves, J. A. Carvalho, Z. M. Lima, and J. M. Sasaki, "Size-strain study of NiO nanoparticles by X-ray powder diffraction line broadening," *Materials Letters*, vol. 72, pp. 36–38, 2012.
- [17] C. R. Bhunya and H. C. Padhi, "Alloying effect on the K_{beta}/K_{alpha} intensity ratios of Ti, Cr and Ni," *Journal of Physics B: Atomic, Molecular and Optical Physics*, vol. 25, no. 24, pp. 5283–5287, 1992.
- [18] Y. Li, D.-S. Hwang, N. H. Lee, and S.-J. Kim, "Synthesis and characterization of carbon-doped titania as an artificial solar

- light sensitive photocatalyst," *Chemical Physics Letters*, vol. 404, no. 1-3, pp. 25–29, 2005.
- [19] H. H. Pham and L.-W. Wang, "Oxygen vacancy and hole conduction in amorphous TiO_2 ," *Physical Chemistry Chemical Physics*, vol. 17, no. 1, pp. 541–550, 2015.
- [20] L. Qin, Q. Chen, R. Lan et al., "Effect of anodization parameters on morphology and photocatalysis properties of TiO_2 nanotube arrays," *Journal of Materials Science & Technology*, vol. 31, no. 10, pp. 1059–1064, 2015.
- [21] M. Erol, T. Dikici, M. Toparli, and E. Celik, "The effect of anodization parameters on the formation of nanoporous TiO_2 layers and their photocatalytic activities," *Journal of Alloys and Compounds*, vol. 604, pp. 66–72, 2014.
- [22] R. Beranek, H. Tsuchiya, T. Sugishima et al., "Enhancement and limits of the photoelectrochemical response from anodic TiO_2 nanotubes," *Applied Physics Letters*, vol. 87, no. 24, article 243114, 2005.
- [23] H. Tang, K. Prasad, R. Sanjinès, P. E. Schmid, and F. Lévy, "Electrical and optical properties of TiO_2 anatase thin films," *Journal of Applied Physics*, vol. 75, no. 4, pp. 2042–2047, 1994.
- [24] A. R. Newmark and U. Stimming, "Photoelectrochemical studies of passive films on zirconium and amorphous iron-zirconium alloys," *Langmuir*, vol. 3, no. 6, pp. 905–910, 1987.
- [25] R. M. Hill, "Poole-Frenkel conduction in amorphous solids," *Philosophical Magazine*, vol. 23, no. 181, pp. 59–86, 1971.
- [26] J. L. Hartke, "The three-dimensional Poole-Frenkel effect," *Journal of Applied Physics*, vol. 39, no. 10, pp. 4871–4873, 1968.
- [27] Y. Mukouyama, S. Nakanishi, H. Konishi, Y. Ikeshima, and Y. Nakato, "New-type electrochemical oscillation caused by electrode–surface inhomogeneity and electrical coupling as well as solution stirring through electrochemical gas evolution reaction," *The Journal of Physical Chemistry B*, vol. 105, no. 44, pp. 10905–10911, 2001.
- [28] J. Keizer and D. Scherson, "A theoretical investigation of electrode oscillations," *The Journal of Physical Chemistry*, vol. 84, no. 16, pp. 2025–2032, 1980.

